

Anderson transitions : multifractal or non-multifractal statistics of the transmission as a function of the scattering geometry

Cecile Monthus and Thomas Garel

Institut de Physique Theorique, CNRS and CEA Saclay 91191 Gif-sur-Yvette cedex, France

The scaling theory of Anderson localization is based on a global conductance g_L that remains a random variable of order $O(1)$ at criticality. One realization of such a conductance is the Landauer transmission form any transverse channels. On the other hand, the statistics of the one-channel Landauer transmission between two local probes is described by a multifractal spectrum that can be related to the singularity spectrum of individual eigenstates. To better understand the relations between these two types of results, we consider various scattering geometries that interpolate between these two cases and analyse the statistics of the corresponding transmissions. We present detailed numerical results for the power-law random banded matrices (PRBM) model. Our conclusions are : (i) in the presence of one isolated incoming wire and many outgoing wires, the transmission has the same multifractal statistics as the local density of states of the site where the incoming wire arrives; (ii) in the presence of backward scattering channels with respect to the case (i), the statistics of the transmission is not multifractal anymore, but becomes monofractal. Finally, we also describe how these scattering geometries influence the statistics of the transmission at criticality.

I. INTRODUCTION

Within the field of Anderson localization [1] (see the reviews [2, 3, 4, 5, 6, 7, 8]), one main achievement has been the formulation of a scaling theory [9] describing the renormalization flow of the typical global conductance g_L as a function of the linear size L of the system. The critical point then corresponds to a finite conductance, whereas the delocalized phase corresponds to the growing RG flow $g_L \sim L^{d-2}$ in dimension $d > 2$, and the localized phase corresponds to the decaying RG flow $g_L \sim e^{-(cst)L}$. Although this scaling theory was first formulated in terms of the Thouless definition of conductance, based on the sensitivity to boundary conditions, it was then realized that a more straightforward definition of a global conductance can be obtained via the quantum scattering theory where the quantum transmission $T_L^{m \rightarrow c}$ is given by the many-channel (m.c.) Landauer formula [10, 11, 12, 13] that generalizes the one-dimensional case [14, 15, 16].

This scattering definition has the advantage to have a well defined meaning for each disordered sample, and thus one may study its probability distribution over the samples [10] (see [7] for a review of the results concerning this distribution both in the localized phase and at criticality). From the point of view of the scaling theory, the important point is that at criticality, the many-channel Landauer transmission $T_L^{m \rightarrow c}$ remains a random variable of order $O(1)$ as $L \rightarrow \infty$. On the other hand, it is now well established that individual critical eigenfunctions are multifractal (see the reviews [6, 8]). As a consequence, the one-channel Landauer transmission $T_L^{(1;1)}$ between two local probes is expected to display also multifractal properties at criticality [17, 18, 19]. To better understand the relation between this multifractal statistics of the one-channel Landauer transmission $T_L^{(1;1)}$ and the many-channel Landauer transmission $T_L^{m \rightarrow c}$, we consider in this paper various scattering geometries that interpolate between the two in order to characterize the statistics of the transmission in these intermediate conditions. We present detailed numerical results for the Anderson critical points of the Power-law Random Banded Matrix (PRBM) model, where the criticality condition is exactly known.

The paper is organized as follows. In section II, we recall the definition and some properties of the PRBM model. We then consider the statistics of the transmission at criticality for the following scattering geometries :

- one incoming wire and one outgoing wire (section III)
- one incoming wire and many outgoing wires (section IV)
- one incoming wire with many backward channels and many outgoing wires (section V)

For completeness in section VI, we describe how these scattering geometries influence the statistics of the transmission at criticality. Our conclusions are summarized in section VII. A brief reminder on multifractality of critical eigenfunctions is given in Appendix A.

II. REMINDER ON THE POWER-LAW RANDOM BANDED MATRIX (PRBM) MODEL

Beside the usual short-range Anderson tight-binding model in finite dimension d , other models displaying Anderson localization have been studied, in particular the Power-law Random Banded Matrix (PRBM) model, which can be viewed as a one-dimensional model with long-ranged random hopping decaying as a power-law $(b-r)^{\alpha}$ of the distance

with exponent a and parameter b . Many properties of the Anderson transition at $a = 1$ between localized states with integrable power-law tails ($a > 1$) and extended states ($a < 1$) have been studied, in particular the statistics of eigenvalues [21, 22, 23], and the multifractality of eigenfunctions [24, 25, 26, 27, 28, 29], including boundary multifractality [30]. The critical properties at $a = 1$ depend continuously on the parameter b , which plays a role analogous to the dimension d in short-range Anderson transitions [24]: the limit $b \rightarrow 1$ corresponds to weak multifractality (analogous to the case $d = 2+$) and can be studied via the mapping onto a non-linear sigma model [20], whereas the case $b \rightarrow \infty$ corresponds to strong multifractality (analogous to the case of high dimension d) and can be studied via Levitov renormalization [24, 32]. Other values of b have been studied numerically [24, 25, 26, 27]. The statistics of scattering phases, Wigner delay times and resonance widths in the presence of one external wire have been discussed in [31, 33]. Related studies concern dynamical aspects [34], the case with no on-site energies [35], and the case of power-law hopping terms in dimension $d > 1$ [36, 37, 38].

In this paper, we consider the PRBM in dimension $d = 1$ either in the line geometry with two boundaries or in the ring geometry with periodic boundary conditions, in the presence of various external wires to measure the transmission properties.

A. PRBM with boundaries (line geometry)

In the line geometry, the distance $r_{i,j}$ between two sites (i, j) is simply

$$r_{i,j} = |i - j| \quad (1)$$

The ensemble of power-law random banded matrices of size $L \times L$ is then defined as follows: the matrix elements $H_{i,j}$ are independent Gaussian variables of zero-mean $\overline{H_{i,j}} = 0$ and of variance

$$\overline{H_{i,j}^2} = \frac{1}{1 + \frac{r_{i,j}^{2a}}{b}} \quad (2)$$

B. PRBM with periodic boundary conditions (ring geometry)

In the ring geometry with periodic boundary conditions, the appropriate distance $r_{i,j}$ between the sites i and j on a ring of L sites is defined as [24]

$$r_{i,j}^{(L)} = \frac{L}{2\pi} \sin^{-1} \left(\frac{i - j}{L} \right) \quad (3)$$

The matrix elements $H_{i,j}$ are then defined as before in terms of this distance (Eq. 2). The main property of this ring geometry is that all sites are equivalent, whereas in the line geometry there are two boundaries at $i = 1$ and at $i = L$.

C. Scattering transmission in the presence of external wires

In the following, we will consider various scattering geometries, where the disordered sample is linked to one incoming wire, parametrized by the half-line $(x \rightarrow x^{\text{in}})$, and to one or many outgoing wires, parametrized by the half-lines $(x_j \rightarrow x_j^{\text{out}})$. In each case, we are interested in the eigenstate $|j\rangle$ that satisfies the Schrödinger equation

$$H |j\rangle = E |j\rangle \quad (4)$$

inside the disorder sample characterized by the random $H_{i,j}$, and in the perfect wires characterized by no on-site energy and by hopping unity between nearest neighbors. Within these perfect wires, one requires the plane-wave forms

$$\begin{aligned} \psi_{\text{in}}(x \rightarrow x^{\text{in}}) &= e^{ik(x - x^{\text{in}})} + r e^{-ik(x - x^{\text{in}})} \\ \psi_{\text{out}}(x_j \rightarrow x_j^{\text{out}}) &= t_j e^{ik(x_j - x_j^{\text{out}})} \end{aligned} \quad (5)$$

These boundary conditions define the reflection amplitude r of the incoming wire and the transmission amplitudes (t_j) of the outgoing wires.

The Landauer transmission T of a subset J of the outgoing wires defined as

$$T(J) = \frac{1}{|J|} \sum_{j \in J} |t_j|^2 \quad (6)$$

is then a number in the interval $[0;1]$. The various scattering geometries considered below differ in the number of the possible out-going wires and in the subset J used to measure the transmission.

To satisfy the Schrodinger Eq. 4 within the wires described by Eq. 5, one has the following relation between the energy E and the wave vector k

$$E = 2 \cos k \quad (7)$$

To simplify the discussion, we will focus in this paper on the case of zero-energy $E = 0$ (wave-vector $k = \pi/2$) that corresponds to the center of the band.

In the following, we study numerically the statistical properties of the Landauer transmission T for systems of sizes $50 \leq L \leq 1800$ with corresponding statistics of $10^4 \leq n_s(L) \leq 2400$ independent samples. For typical values, the number $n_s(L)$ of samples is sufficient even for the bigger sizes, whereas for the measure of multifractal spectrum, we have used only the smaller sizes where the statistics of samples was sufficient to measure correctly the rare events. To measure numerically multifractal spectra, we have used the standard method based on q-measures of Ref. [39] (see Appendix B of [19] for more details).

III. STATISTICS OF THE ONE-CHANNEL TRANSMISSION $T_L^{(1;1)}$

A. Scattering geometry

The one-channel transmission $T_L^{(1;1)}$ is the Landauer transmission when the disordered sample is connected to one incoming wire and one outgoing wire, see Fig. 1 for the case of the PRBM model. This one-channel transmission $T_L^{(1;1)}$ is a very interesting observable to characterize Anderson transitions [17, 18]: (i) it remains finite in the thermodynamic limit only in the delocalized phase, so that it represents an appropriate order parameter for the conducting/non-conducting transition; (ii) exactly at criticality, it displays multifractal properties in direct correspondence with the multifractality of critical eigenstates, i.e. it displays strong fluctuations that are not captured by more global definitions of conductance.

B. Multifractal statistics of $T_L^{(1;1)}$ at criticality

As first discussed in [17] for the special case of the two dimensional quantum Hall transition, the critical probability distribution of the one-channel transmission $T_L^{(1;1)}$ is described by a multifractal spectrum $\chi^{(1;1)}(q)$

$$\text{Prob } T_L^{(1;1)} \in [L^{-1}, L] \sim dT_L^{(1;1)} / L^{\chi^{(1;1)}(q)} \quad (8)$$

Its moments involve non-trivial exponents $X^{(1;1)}(q)$

$$\frac{1}{T_L^{(1;1)q}} \sim \int_{L^{-1}}^1 dT_L^{(1;1)} T_L^{\chi^{(1;1)}(q)} \quad (9)$$

that can be computed via the saddle-point in

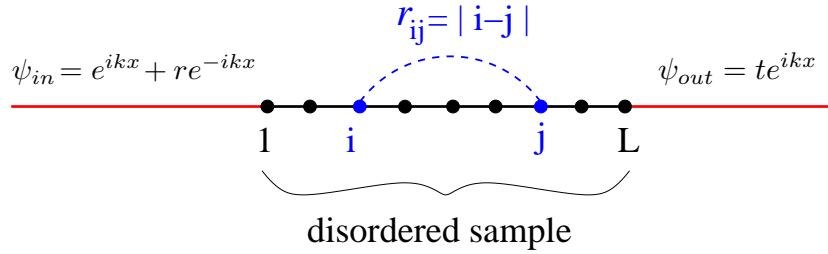
$$X^{(1;1)}(q) = \max_{\chi} \left[\chi^{(1;1)}(q) - q \chi \right] \quad (10)$$

As stressed in [17], the physical bound $T_L^{(1;1)} \leq 1$ on the transmission implies that the multifractal spectrum exists only for $q \geq 0$, and this termination at $q = 0$ leads to a complete freezing of the moments exponents

$$X^{(1;1)}(q) = X^{(1;1)}(q_{\text{sat}}) \quad \text{for } q \geq q_{\text{sat}} \quad (11)$$

at the value q_{sat} where the saddle-point of the integral of Eq. 9 vanishes ($q - q_{\text{sat}} = 0$).

(a) Line geometry



(b) Ring geometry

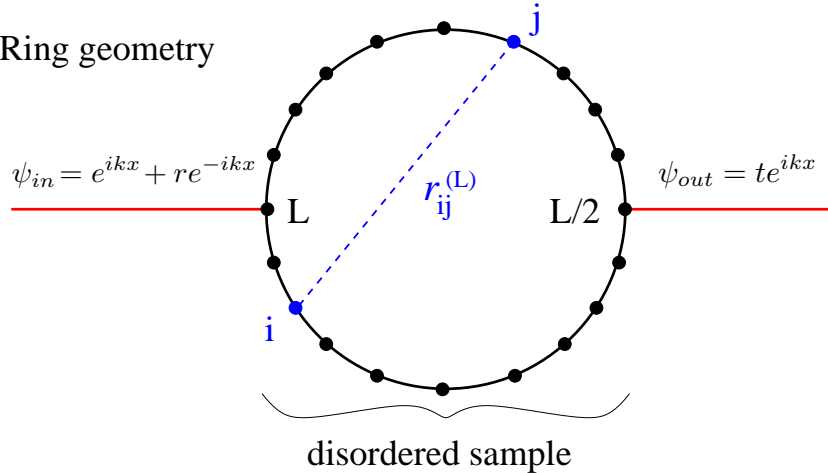


FIG. 1: Scattering geometries defining the one-channel transmission $T_L^{(1;1)}$. (a) Line geometry: the incoming wire is attached to site 1, and the outgoing wire to site L . These two sites are 'boundary sites' for the disordered sample (they have less neighbors than bulk sites). (b) Ring geometry: the incoming wire is attached to site L , and the outgoing wire to site $L/2$. In the ring geometry, all sites are 'bulk sites' for the disordered sample (all sites have the same number of neighbors).

It is very natural to expect that $X^{(1;1)}(\omega)$ is related to the multifractal spectrum $f(\omega)$ concerning eigenfunctions (see the Appendix A for a brief reminder). The possibility proposed in [17] is that before the freezing of Eq. 11 occurs, the transmission should scale as the product of two independent local densities of states (Eq. A 6)

$$X^{(1;1)}(\omega) = 2^{-\omega} \text{ for } \omega < \omega_{\text{sat}} \quad (12)$$

We refer to [17] for physical arguments in favor of this relation. Equations 11 and 12 for the moments exponents are equivalent to following relation between the two multifractal spectra

$$X^{(1;1)}(\omega) = 2^{-\omega} f(\omega) = d + \frac{\omega}{2} \quad (13)$$

In particular, the typical transmission

$$T_L^{\text{typ}} \sim e^{-\ln T_L} \quad (14)$$

is expected to decay at criticality with some power-law

$$T_L^{\text{typ}} \sim L^{-\frac{1}{L} \frac{1}{\omega_{\text{typ}}^{(1;1)}}} \quad (15)$$

where the exponent $\frac{1}{\omega_{\text{typ}}^{(1;1)}}$ is the point where $X^{(1;1)}(\omega)$ reaches its maximum $X^{(1;1)}(\omega_{\text{typ}}^{(1;1)}) = 0$. From Eq. 13, it is

$$\frac{1}{\omega_{\text{typ}}^{(1;1)}} = 2(\omega_{\text{typ}} - d) \quad (16)$$

to the typical exponent τ_{typ} that characterizes the typical weight of eigenfunctions

$$j(\tau) \approx \frac{1}{L^{\tau_{\text{typ}}}} \quad (17)$$

In our recent work [19], we have tested in detail these predictions for the statistics of the one-channel transmission $T_L^{(1;1)}$ for the Power-law Random Banded Matrix (PRBM) model where $d = 1$ in the ring geometry (see the scattering geometry (b) of Figure 1), where all sites are 'bulk sites'. We thus refer the reader to [19] for detailed numerical data.

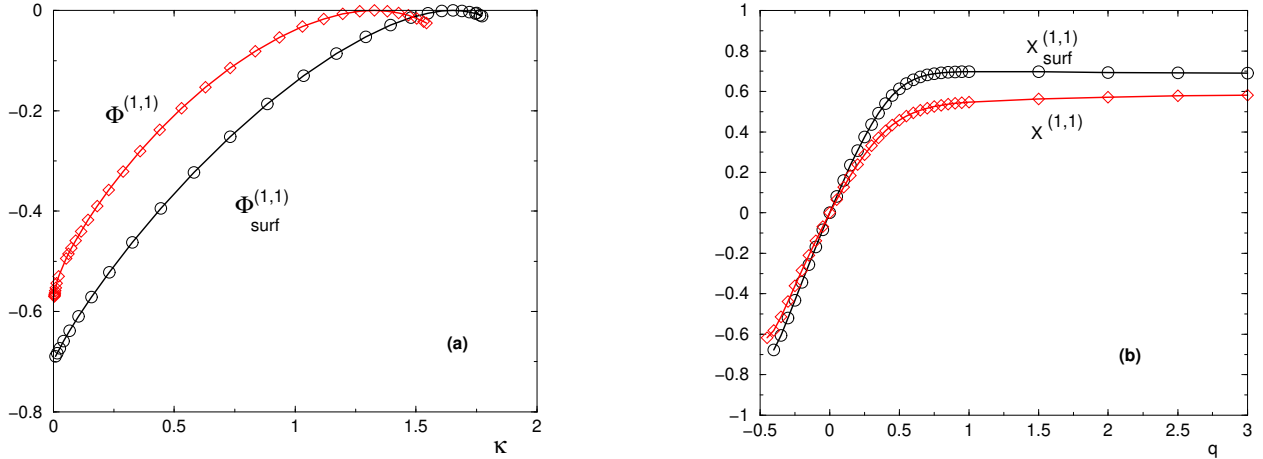


FIG. 2: Multifractal statistics of the one-channel transmission $T_L^{(1;1)}$ for $b = 0.1$ at criticality $a = 1$ for the line geometry and for the ring geometry (see Fig. 1) (a) the multifractal spectra $f^{(1;1)}(q)$ corresponding to the Ring geometry and $f_{\text{surf}}^{(1;1)}(q)$ corresponding to the Line geometry are maximal at the typical values $\tau_{\text{typ}}^{(1;1)} \approx 1.33$ and $\tau_{\text{surf}}^{(1;1)} \approx 1.64$. (b) the corresponding moments exponents $X^{(1;1)}(q)$ and $X_{\text{surf}}^{(1;1)}(q)$ saturate at the values $X^{(1;1)}(q \rightarrow \infty) = X_{\text{sat}}^{(1;1)} \approx 0.58$ and $X_{\text{surf}}^{(1;1)}(q \rightarrow \infty) = X_{\text{surf}}^{(1;1)} \approx 0.69$.

However, in other localization models it is usual to attach leads to the boundaries of the disordered samples. It is thus interesting to consider also the scattering geometry (a) of Figure 1 where the incoming wire and outgoing wire are attached at boundary points, since one expects that at criticality, boundary points are characterized by a different multifractal spectrum $f_{\text{surf}}^{(1;1)}(q)$ [40, 41, 42]. One then expects that the relation of Eq. 13 becomes

$$f_{\text{surf}}^{(1;1)}(q) = \frac{h}{2} f_{\text{surf}}^{(1;1)}(q) = \frac{d + \frac{1}{2}}{d_s} \quad (18)$$

when the transition is measured between two boundary points, where d is the bulk dimension and d_s is the surface dimension. Here the line geometry (a) of Figure 1 corresponds to $d = 1$ and $d_s = 0$. On Fig. 2, we compare for the case $b = 0.1$ at criticality $a = 1$ the bulk multifractal spectrum $f^{(1;1)}(q)$ and the surface multifractal spectrum $f_{\text{surf}}^{(1;1)}(q)$. We find in particular that the typical exponent for the surface case $\tau_{\text{typ}}^{(1;1)\text{surf}}(b = 0.1) \approx 1.64$ coincides numerically with the typical value of the bulk case $\tau_{\text{typ}}^{(1;1)}(b = 0.05) \approx 1.64$ measured in [19]. This is in agreement with Eq. 29 of Ref. [41] stating that in the regime of small b , the surface multifractal spectrum of parameter b coincides with the bulk multifractal spectrum of parameter $b=2$ (here we consider the case $p = 0$ in the notations of Ref. [41]).

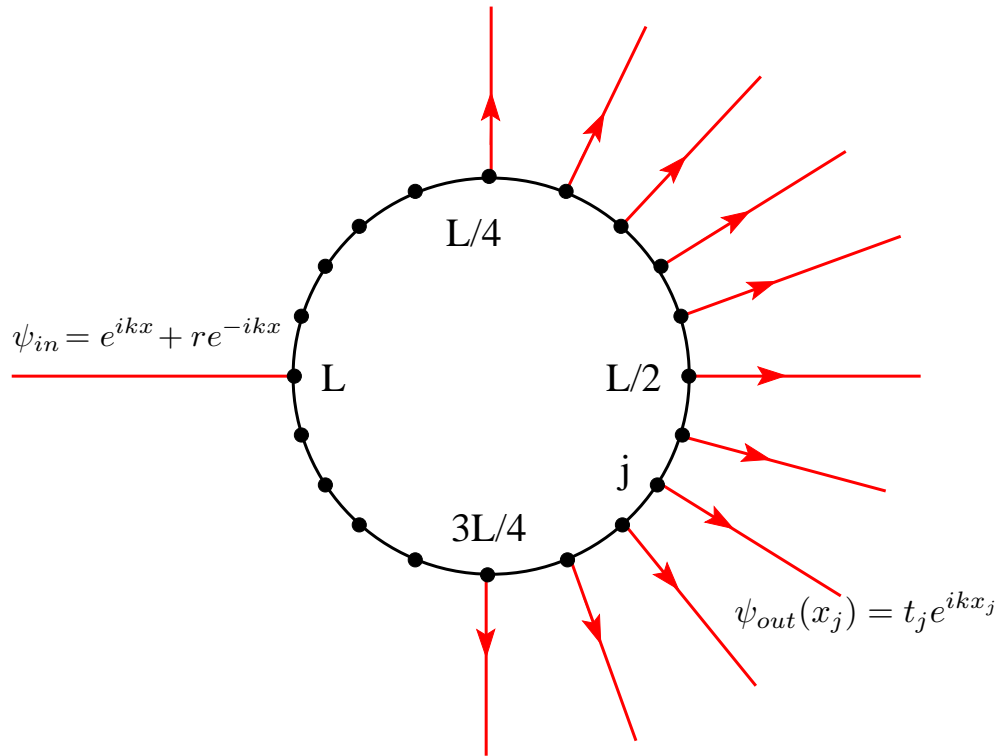


FIG. 3: Scattering geometry defining the 'one-to-many' transmission $T_L^{(1;m)}$ for the Ring geometry: the incoming wire is attached to site L , and outgoing wires are attached at all sites j satisfying $L/4 \leq j \leq 3L/4$. The total transmission is given by Eq. 19 in terms of the amplitudes t_j of the outgoing wires and of the reflection amplitude r of the incoming wire.

IV. STATISTICS OF THE ONE-TO-MANY-CHANNEL TRANSMISSION $T_L^{(1;m)}$

A. Scattering geometry

We now consider the scattering geometry of Fig. 3 where the incoming wire is attached to site $i = L$, and where there are $(L/2 + 1)$ outgoing wires attached to the sites $j = L/4; L/4 + 1; \dots; 3L/4$. We are interested in the transmission

$$T_L^{(1;m)} = \sum_{j=L/4}^{3L/4} |t_j|^2 = 1 - |r|^2 \quad (19)$$

where the t_j are the transmission amplitudes and where r is the reflection amplitude of the incoming wire (Eqs 5).

B. Multifractal statistics of $T_L^{(1;m)}$ at criticality

In this scattering geometry, one expects that the critical statistics is still multifractal with a spectrum $X^{(1;m)}(\alpha)$

$$\text{Prob } T_L^{(1;m)} \in [L^{-\alpha}, L^{-\alpha+1}] \sim L^{-X^{(1;m)}(\alpha)} \quad (20)$$

and non-trivial exponents $X^{(1;m)}(\alpha)$

$$\frac{1}{T_L^{(1;m)^\alpha}} \sim \int_{L^{-\alpha}}^{L^{-\alpha+1}} dL^{-\alpha} L^{-\alpha} L^{-X^{(1;m)}(\alpha)} \quad (21)$$

Again the physical bound $T_L^{(1;m)} \leq 1$ on the transmission implies that the multifractal spectrum exists only for $\alpha \geq 0$, and this termination at $\alpha = 0$ leads to a complete freezing of the moments exponents

$$X^{(1;m)}(\alpha) = X^{(1;m)}(\alpha_{\text{sat}}) \quad \text{for } \alpha \geq \alpha_{\text{sat}} \quad (22)$$

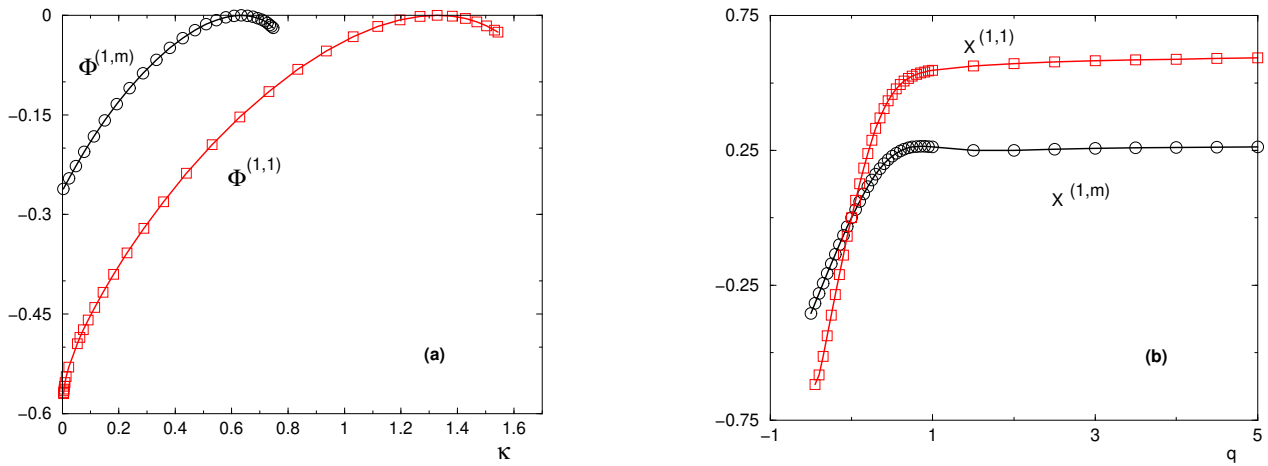


FIG. 4: Multifractal statistics of the one-to-m any transmission for $b = 0.1$ at criticality $a = 1$ for the scattering geometry of Fig. 3 (a) the multifractal spectrum $\Phi^{(1,m)}(\kappa)$ () as compared to the multifractal spectrum $\Phi^{(1,1)}(\kappa)$ (). The typical values $\kappa_{typ}^{(1,m)} = 0.66$ and $\kappa_{typ}^{(1,1)} = 1.32$ satisfy the relation of Eq. 26. The termination values $\Phi^{(1,m)}(0) = 0.27$ and $\Phi^{(1,1)}(0) = 0.58$ satisfy the relation of Eq. 27. The full relation between the two multifractal spectra is given by Eq. 25. (b) the corresponding moments exponents $X^{(1,m)}(q)$ () as compared to $X^{(1,1)}(q)$ ().

at the value q_{sat} where the saddle-point of the integral of Eq. 21 vanishes ($q = q_{sat}$) = 0. However in the presence of many wires (m more precisely, whenever the number of outgoing wires is greater than $L^{(1,1)}(\kappa=0)=2$ according to the discussion of the previous section), one expects that the relation of Eq. 12 becomes

$$X^{(1,m)}(q) = (q) \text{ for } q \geq q_{sat} \quad (23)$$

meaning that the transmission simply scales as the local density of states seen by the incoming wire. Equations 22 and 23 for the moments exponents are equivalent to following relation with the eigenfunction singularity spectrum $f(\kappa)$

$$\Phi^{(1,m)}(\kappa) = f(\kappa) \quad (24)$$

Equivalently using Eq. 13, one obtains the simple relation

$$\Phi^{(1,m)}(\kappa) = \frac{\Phi^{(1,1)}(\kappa)}{2} \quad (25)$$

In particular, the typical values of κ (where the spectra reach their maximal value 0) are related by

$$\kappa_{typ}^{(1,m)} = \frac{\kappa_{typ}^{(1,1)}}{2} \quad (26)$$

The termination values at $\kappa = 0$ are also related by the simple relation

$$\Phi^{(1,m)}(0) = \frac{\Phi^{(1,1)}(0)}{2} \quad (27)$$

We have checked these relations (Eqs 25, 26, 27) for the case $b = 0.1$ at criticality $a = 1$ (see Fig. 4).

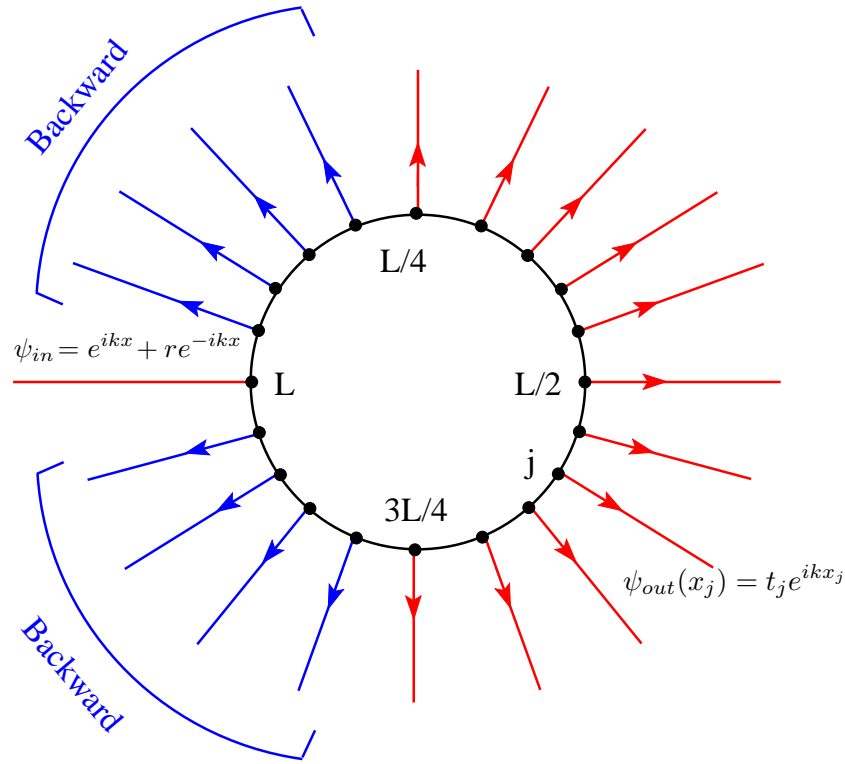


FIG. 5: Scattering geometry defining the ‘one-to-many’ transmission $T_L^{(1B, m)}$ in the presence of backward channels: in addition to Fig. 3, there are now outgoing wires for $1 \leq j < L/4$ and $3L/4 < j \leq L-1$ that are considered as backward scattering channels. The total transmission is given by Eq. 28 in terms of the amplitudes t_j of the outgoing wires for $L/4 \leq j \leq 3L/4$.

V. STATISTICS OF THE ONE-TO-MANY-CHANNEL TRANSMISSION $T_L^{(1B, m)}$ IN THE PRESENCE OF BACKWARD CHANNELS

A. Scattering geometry

We now consider the scattering geometry of Fig. 5: the only difference with the previous case of Fig. 3 is the presence of backward scattering channels near the incoming wire. We are interested into the transmission

$$T_L^{(1B, m)} = \sum_{j=L/4}^{3L/4} |t_j|^2 \quad (28)$$

where the t_j are the transmission amplitudes (Eqs 5).

B. Non-multifractal statistics at criticality

In this case, we find numerically that the statistics of the transmission is not multifractal anymore, but monofractal

$$T_L^{(1B, m)} \sim \frac{1}{L^{\text{back}}} \quad (29)$$

where back is a random variable of order $O(1)$. Moreover, the monofractal exponent is

$$\text{back}(b) = 1 \quad \text{for all } b \quad (30)$$

as shown on Fig. 6 for the three values $b = 0.01$, $b = 0.1$ and $b = 0.25$, i.e. it does not depend anymore on the multifractal critical properties that are known to change continuously with the parameter b in the PRBM. For instance for the one-channel transmission, we have measured in [19] the typical exponents $\text{typ}^{(1;1)}(b = 0.01) = 1.92$, $\text{typ}^{(1;1)}(b = 0.1) = 1.33$, and $\text{typ}^{(1;1)}(b = 0.25) = 0.77$ which are significantly different.

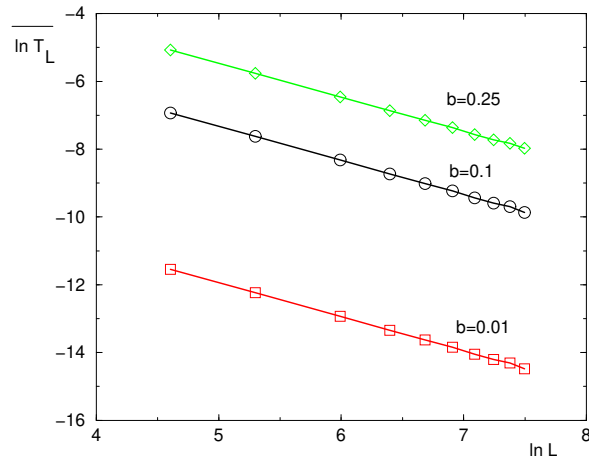


FIG. 6: Statistics of the transmission $T_L^{(1B^m)}$ for the scattering geometry of Fig. 5 at criticality $a = 1 : \ln T_L^{\text{typ}}$ as a function of $\ln L$. The slopes for the three values $b = 0.01, b = 0.1$ and $b = 0.25$ coincide $b_{\text{back}}(b) = 1$ (see Eq. 30).

C. Consequences for the usual many-channel (m.c.) transmission $T_L^{m.c.}$

For the short-range Anderson tight-binding model in dimension $d = 3$, the usual many-channel Landauer transmission $T_L^{m.c.}$ corresponds to the incoherent sum

$$T_L^{m.c.} = \sum_{i \in L^{d_s}} T_i \quad (31)$$

of $L^{d_s} = L^{d-1}$ contributions T_i , where T_i is the coherent scattering transmission for one incoming wire arriving at i , with L^{d_s} backward scattering channels and with L^{d_s} forward scattering channels (see for instance Fig. 2 of Ref [12]). The statistics of this many-channel transmission has been much studied (see the review [7]): $T_L^{m.c.}$ is a random variable of order $O(1)$. One of our motivations for the present study was to determine whether the statistics of each contribution T_i was multifractal or not. Since each contribution T_i is analog to the transmission of scattering geometry of Fig. 5, our present study suggests that each contribution T_i in the incoherent sum of Eq. 31 is not multifractal, but monofractal with an exponent $b_{\text{back}} = d_s = d - 1$ in short-range models, i.e. this exponent does not depend on the critical multifractal spectrum.

VI. INFLUENCE OF THE SCATTERING GEOMETRY ON THE TRANSMISSION OFF CRITICALITY

Up to now, we have only discussed the transmission statistics at criticality. For completeness, we briefly describe in this section how the behavior of the transmission depends on the scattering geometry outside criticality.

A. Influence of the scattering geometry in the localized phase

In usual short-range models, the localized phase is characterized by exponentially localized wavefunctions, whereas in the presence of power-law hoppings, localized wavefunction can only decay with power-law integrable tails. For the PRBM, it is moreover expected that the asymptotic decay is actually given exactly by the power-law of Eq. 2 for the hopping term defining the model [20]:

$$j(r) \stackrel{p}{\sim} \frac{1}{r^{2a}} \quad (32)$$

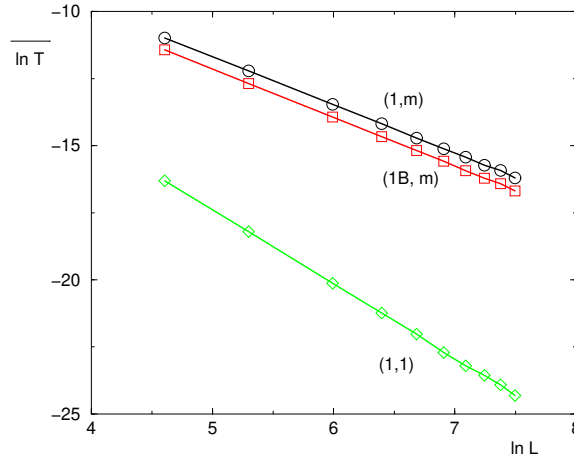


FIG. 7: Statistics of the transmissions $T_L^{(1;1)}$, $T_L^{(1;m)}$ and $T_L^{(1B;m)}$ for the scattering geometries of Fig. 1, 3 and 5 in the localized phase $a = 1.4$ for $b = 0.1$: the measured slopes on this log-log plot are in agreement with Eq. 33.

As a consequence in the localized phase $a > 1$, one expects the following typical decays for the transmissions $T_L^{(1;1)}$, $T_L^{(1;m)}$ and $T_L^{(1B;m)}$ for the scattering geometries of Fig. 1, 3 and 5

$$\begin{aligned} \overline{\ln T_L^{(1;1)}} (a > 1) & \sim \frac{1}{L^{1/1}} \sim 2a \ln L \\ \overline{\ln T_L^{(1;m)}} (a > 1) & \sim \frac{1}{L^{1/1}} \sim (2a - 1) \ln L \\ \overline{\ln T_L^{(1B;m)}} (a > 1) & \sim \frac{1}{L^{1/1}} \sim (2a - 1) \ln L \end{aligned} \quad (33)$$

The decay of $T_L^{(1;1)}$ directly reflects the decay of Eq. 32 of wavefunctions. The presence of many outgoing channels change the power by one as a consequence of the integration over all the sites connected to outgoing channels. And the presence of backward channels does not change this exponent. This is in agreement with our numerical results shown on Fig. 7 for the case $a = 1.4$ and $b = 0.1$. We refer to our previous work [19] for more details on the histogram around the typical value for the one-channel case.

B. Influence of the scattering geometry in the delocalized phase

In the delocalized phase, the eigenfunctions are not multifractal, but monofractal with the single value $\nu_{\text{deloc}} = d$ for the weight $j_L^2(x)j$. As a consequence, the typical transmission for the one-channel case of Fig. 1 is expected to remain finite as $L \rightarrow \infty$ [17] (in Eq. 16, the case $\nu_{\text{typ}} = d$ yields $\nu_{\text{typ}} = 0$)

$$T_L^{(1;1)} (a < 1) \sim \frac{1}{L^{1/1}} \quad T_1^{(1;1)} > 0 \quad (34)$$

The one-channel transmission is thus a good order parameter of the transport properties [17]. We refer to our previous work [19] for more details on the histogram for this one-channel case. In the presence of many outgoing wires as in Fig. 3, the transmission will thus also remain finite

$$T_L^{(1;m)} (a < 1) \sim \frac{1}{L^{1/1}} \quad T_1^{(1;m)} > 0 \quad (35)$$

However in the presence of backward scattering channels as in Fig. 5, one expects that the transmission will now decay with L . For instance in the usual short-range Anderson model in dimension $d = 3$, the many-channel transmission of Eq. 31 scales as L^{d-2} , i.e. each contribution T_i in the presence of backward channels scales as $1/L$, which represents the probability to reach first the out-going surface without returning to the incoming surface for a diffusive particle. For the PRBM, our numerical results indicate the typical decay

$$\overline{\ln T_L^{(1B;m)}} (a < 1) \sim \frac{1}{L^{1/1}} \sim (2a - 1) \ln L \quad (36)$$

which corresponds to the probability to make a direct hopping towards a forward channel without visiting the sites connected to the backward channels.

VII. CONCLUSION

In this paper, we have studied how the scattering geometry determines the statistics of the Landauer transmission, both at criticality and outside criticality. We have presented detailed numerical results for the PRBM model for various scattering geometries that interpolate between the two cases that are usually considered, namely the one-channel and the many-channel cases. We have found that : (i) in the presence of one isolated incoming wire and many outgoing wires, the transmission has the same multifractal statistics as the local density of states of the site where the incoming wire arrives; (ii) in the presence of backward scattering channels with respect to the case (i), the statistics of the transmission is not multifractal anymore, but becomes monofractal.

APPENDIX A : REMINDER ON MULTIFRACTALITY OF EIGENFUNCTIONS

In this Appendix, we recall some useful properties concerning eigenfunction multifractality. The multifractal spectrum $f(\cdot)$ is defined as follows (for more details see for instance the reviews [6, 8]): in a sample of size L^d , the number $N_L(\cdot)$ of points \mathbf{x} where the weight $j(\mathbf{x})^2$ scales as $L^{-\cdot}$ behaves as

$$N_L(\cdot) \sim L^{f(\cdot)} \quad (\text{A 1})$$

The typical value \cdot_{typ} corresponds to the maximum value $f(\cdot_{\text{typ}}) = d$ of the multifractal spectrum $f(\cdot)$. The inverse participation ratios (IPR.s) can be then rewritten as an integral over

$$Y_q(L) = \int_{L^d} d^d \mathbf{x} j(\mathbf{x})^{2q} \sim \int_{L^d} d^d \mathbf{x} L^{-q f(\cdot)} \sim L^{-q \cdot} \quad (\text{A 2})$$

The exponent $\cdot(q)$ can be obtained via a saddle-point calculation in \cdot , and one obtains the Legendre transform formula [6, 8]

$$\begin{aligned} \cdot(q) &= f'(\cdot) \\ (q) &= q - f(\cdot) \end{aligned} \quad (\text{A 3})$$

These scaling behaviors, which concern individual eigenstates ψ_n , can be translated for the local density of states

$$\rho_L(E; \mathbf{x}) = \sum_n \delta(E - E_n) |j_{E_n}(\mathbf{x})|^2 \quad (\text{A 4})$$

as follows : for large L , when the L^d energy levels become dense, the sum of Eq. A 4 scales as

$$\rho_L(E; \mathbf{x}) \sim L^{-q} j_E(\mathbf{x})^2 \quad (\text{A 5})$$

and its moments involve the exponents $\cdot(q)$ introduced in Eq. A 2

$$\overline{[\rho_L(E; \mathbf{x})]^q} \sim \frac{1}{L^{-q \cdot(q)}} \quad \text{with} \quad \cdot(q) = \cdot - d(q - 1) \quad (\text{A 6})$$

These notions concerning bulk multifractality have been recently extended to surface multifractality [40, 41, 42] : the idea is that points near the boundaries are described by another multifractal spectrum $f_{\text{surf}}(\cdot)$ which is in general not simply related to the bulk multifractal spectrum $f(\cdot)$.

-
- [1] P.W. Anderson, Phys. Rev. 109, 1492 (1958).
 - [2] D.J. Thouless, Phys. Rep. 13, 93 (1974) ; D.J. Thouless, in "III Condensed Matter" (Les Houches 1978), Eds R. Balian et al. North-Holland, Amsterdam (1979).
 - [3] B. Souillard, in "Chance and Matter" (Les Houches 1986), Eds J. Souletie et al. North-Holland, Amsterdam (1987).
 - [4] I.M. Lifshitz, S.A. Gredeskul and L.A. Pastur, "Introduction to the theory of disordered systems" (Wiley, NY, 1988).
 - [5] B. Kramer and A. Mackinnon, Rep. Prog. Phys. 56, 1469 (1993).
 - [6] M. Janssen, Phys. Rep. 295, 1 (1998).
 - [7] P. Markos, Acta Physica Slovaca 56, 561 (2006).

- [8] F. Evers and A. D. Mirlin, *Rev. Mod. Phys.* 80, 1355 (2008).
- [9] E. Abraham, P. W. Anderson, D. C. Licciardello and T. V. Ramakrishnan, *Phys. Rev. Lett.* 42, 673 (1979).
- [10] P. W. Anderson, D. J. Thouless, E. Abraham, and D. S. Fisher, *Phys. Rev. B* 22, 3519 (1980); P. W. Anderson, *Phys. Rev. B* 23 4828 (1981).
- [11] D. S. Fisher and P. A. Lee *Phys. Rev. B* 23 6851 (1981).
- [12] M. Buttiker, Y. Imry, R. Landauer, and S. Pincus *Phys. Rev. B* 31 6207 (1985).
- [13] A. D. Stone and A. Szafer, *IBM J. Res. Dev.* 32, 384 (1988).
- [14] R. Landauer, *Philos. Mag.* 21, 863 (1970).
- [15] P. W. Anderson and P. A. Lee, *Suppl. Prog. Theor. Phys.* 69, 212 (1980).
- [16] J. M. Luck, "Systemes desordonnes unidimensionnels", *Acta Saclay* (1992).
- [17] M. Janssen, M. Metzler and M. R. Zimbauer, *Phys. Rev. B* 59, 15836 (1999).
- [18] F. Evers, A. Mildenberger and A. D. Mirlin, *Phys. Stat. Sol.* 245, 284 (2008).
- [19] C. Monthus and T. Garel, *arXiv:0903.1988*.
- [20] A. D. Mirlin et al, *Phys. Rev. E* 54, 3221 (1996).
- [21] I. Varga and D. Braun, *Phys. Rev. B* 61, R11859 (2000).
- [22] V. E. Kravtsov et al, *J. Phys. A* 39, 2021 (2006).
- [23] A. M. Garcia-Garcia, *Phys. Rev. E* 73, 026312 (2006).
- [24] F. Evers and A. D. Mirlin *Phys. Rev. Lett.* 84, 3690 (2000); A. D. Mirlin and F. Evers, *Phys. Rev. B* 62, 7920 (2000).
- [25] E. Cuevas, V. Gasparian and M. Ortuno, *Phys. Rev. Lett.* 87, 056601 (2001).
- [26] E. Cuevas et al, *Phys. Rev. Lett.* 88, 016401 (2001).
- [27] I. Varga, *Phys. Rev. B* 66, 094201 (2002).
- [28] E. Cuevas, *Phys. Rev. B* 68, 024206 (2003).
- [29] A. D. Mirlin et al, *Phys. Rev. Lett* 97, 046803 (2006).
- [30] A. Mildenberger et al, *Phys. Rev. B* 75, 094204 (2007).
- [31] J. A. Mendez-Bernandez and T. Kottos, *Phys. Rev. B* 72, 064108 (2005).
- [32] L. S. Levitov, *Europhys. Lett.* 9, 83 (1989); L. S. Levitov, *Phys. Rev. Lett.* 64, 547 (1990); B. L. Altshuler and L. S. Levitov, *Phys. Rep.* 288, 487 (1997); L. S. Levitov, *Ann. Phys. (Leipzig)* 8, 5, 507 (1999).
- [33] J. A. Mendez-Bernandez and I. Varga, *Phys. Rev. B* 74, 125114 (2006).
- [34] R. P. A. Lima et al, *Phys. Rev. B* 71, 235112 (2005).
- [35] R. P. A. Lima et al, *Phys. Rev. B* 69, 165117 (2004).
- [36] H. Potempa and L. Schweitzer, *Phys. Rev. B* 65, 201105 (R) (2002).
- [37] E. Cuevas, *Phys. Stat. Sol.* 241, 2109 (2004).
- [38] E. Cuevas, *Phys. Rev. B* 71, 024205 (2005).
- [39] A. Chhabra and R. V. Jensen, *Phys. Rev. Lett.* 62, 1327 (1989).
- [40] A. R. Subramaniam, I. A. Gruzberg, A. W. W. Ludwig, F. Evers, A. Mildenberger, and A. D. Mirlin, *Phys. Rev. Lett.* 96, 126802 (2006).
- [41] A. Mildenberger, A. R. Subramaniam, R. Narayanan, F. Evers, I. A. Gruzberg, and A. D. Mirlin, *Phys. Rev. B* 75, 094204 (2007).
- [42] H. Obose, A. R. Subramaniam, A. Furusaki, I. A. Gruzberg, and A. W. W. Ludwig, *Phys. Rev. Lett.* 101, 116802 (2008).